

# Hierarchically Self-Assembled Host-Guest Network at the Solid/Liquid-Interface for Single Molecule Manipulation

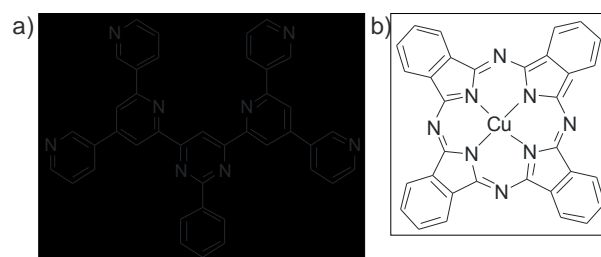
Christoph Meier,<sup>a</sup> Katharina Landfester,<sup>a</sup> Daniela Künzel,<sup>b</sup> Thomas Markert,<sup>b</sup> Axel Groß,<sup>b</sup> and Ulrich Ziener<sup>a\*</sup>

The manufacturing of functional molecular devices is one of the key research topics in nanotechnology. For applications as molecular storage and quantum computing, molecules must be arranged in a repetitive and spatially well ordered structure as well as addressable and manipulable in a controlled fashion. The self-assembly of molecular building blocks with hydrogen bonding capabilities is a suitable method to generate highly ordered and porous two-dimensional (2D) hydrogen bonded networks (HBN).<sup>[1, 2]</sup> Those porous 2D HBNs can be used to immobilise organic and inorganic guest molecules in a spatially well ordered arrangement, predetermined through the host network structure.<sup>[3]</sup> The controlled manipulation of guest molecules was demonstrated for various functional guest molecules by means of scanning tunneling microscopy (STM) experiments, but so far limited to controlled desorption or lateral manipulation of single molecules.<sup>[4-8]</sup> In contrast to UHV conditions where the reservoir of manipulable molecules is restricted to the number of adsorbed species, the supernatant liquid phase at the solid-liquid interface in principle offers an almost unlimited depot of molecules (“ink”) and is therefore the perfect experimental environment for tip-controlled adsorption of guest molecules into the HBN network. The “ink” attribute of a supernatant solution is used in scanning probe based lithographic techniques such as replacement lithography<sup>[9]</sup> and dip-pen lithography<sup>[10]</sup> to tailor the chemical composition and structure of a surface at the sub-100 nm scale length. So far, those lithographic techniques are limited to a resolution of about 15 nm.<sup>[11]</sup>

For a successful spatially controlled adsorption of guest molecules in an HBN, the host-guest system has to fulfil the following requirements: a) the host network needs to be inert towards the manipulation process, b) the dynamics of the manipulated components needs to be slow enough in order to

follow the result of the manipulation with STM and c) the occupation of the cavities with guest molecules should be low to offer unoccupied host cavities. All of the above requirements demand well balanced substrate-substrate and substrate-adsorbate interactions.

Here we present a host-guest network where the demands for a spatially tip controlled single molecule manipulation are fulfilled. After describing the outstanding properties of our host-guest system, we demonstrate the spatially tip controlled de- and adsorption of solvated guest molecules from and into the cavities of the host network. The  $C_{2v}$ -symmetric HBN building block **3,3'-BTP** (scheme 1a) forms a polymorphic supramolecular HBN on highly ordered pyrolytic graphite (HOPG). The porous 2D network was used to generate a hierarchically self-assembled host-guest architecture with copper(II)phthalocyanine (CuPc, scheme 1b) as guest molecule. The occupation of individual HBN cavities with CuPc can be altered with a voltage pulse applied to the tip (“erasing” and “writing”).



**Scheme 1.** a) Chemical sketch of the investigated bis(terpyridine) derivative **3,3'-BTP**. b) Sketch of the investigated guest molecule copper(II)-phthalocyanine CuPc.

As recently reported, the deposition of **3,3'-BTP** from a saturated 1,2,4-trichlorobenzene (TCB) solution ( $1.5 \cdot 10^{-3}$  mol·L<sup>-1</sup>) onto HOPG leads to a densely packed linear structure, stabilised through weak hydrogen bonds between the terminal pyridine rings.<sup>[2]</sup> Deposited from a diluted solution ( $3 \cdot 10^{-5}$  mol·L<sup>-1</sup>), the **3,3'-BTP** molecules self-assemble into a 2D long-range ordered porous nanostructure, further denoted as gearwheel structure (see supp. inf.).<sup>[12]</sup> The gearwheel structure exhibits cavities with an inner diameter of approx. 1.6 nm. After adding a solution of  $1.7 \cdot 10^{-5}$  mol·L<sup>-1</sup> CuPc in TCB to the pre-organised **3,3'-BTP** porous structure, bright spots with a diameter of about 1.4 nm appear in the network (figure 1). The bright spots can be assigned to CuPc molecules randomly immobilised in the cavities of the **3,3'-BTP** network. Those features appear exclusively after addition of a CuPc solution to the gearwheel structure and appear selectively in the cavities of the gearwheel structure. Therefore, the host-guest interaction is exclusively associated with the supramolecularly assembled cavities of the gearwheel

[a] C. Meier, Prof. Dr. K. Landfester, Dr. U. Ziener  
Institute of Organic Chemistry III / Macromolecular Chemistry  
University of Ulm  
Albert-Einstein-Allee 11, D-89081 Ulm, Germany  
Fax: (+49)731-50-22883  
E-mail: ulrich.ziener@uni-ulm.de  
Homepage: <http://www.uni-ulm.de/oc3/index.html>

[b] D. Künzel, T. Markert, Prof. Dr. A. Groß  
Institute of Theoretical Chemistry  
University of Ulm  
Albert-Einstein-Allee 11, D-89081 Ulm, Germany

[\*\*] The authors thank the Deutschen Forschungsgemeinschaft DFG for financial support within the SFB 569 and H. Hoster for the short range order analysis.

Supporting information for this article is available on the WWW under <http://www.angewandte.org> or from the author.

structure and is not due to intermolecular donor-acceptor interactions as reported for e.g. cyclic thiophenes and  $C_{60}$ .<sup>[13]</sup>

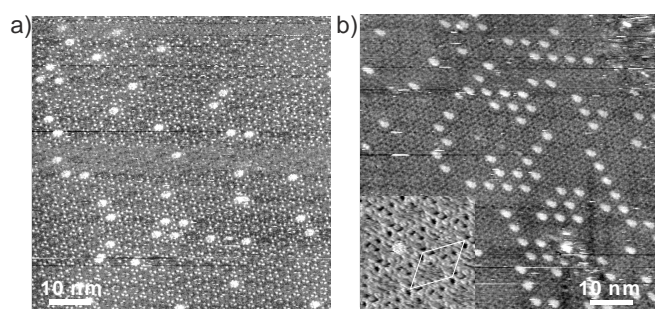


**Figure 1.** a) High resolution STM image of the host-guest network recorded after subsequent addition of CuPc to the **3,3'-BTP** network. The host network is imaged with inverse image contrast due to the applied tunneling conditions. b) Host-guest network after a second addition of CuPc solution to the network in a). The inset (11 nm x 11 nm) shows one occupied cavity and the rhombic unit cell of the host network.

It is noteworthy to mention that the unit cell does not change upon incorporation of the CuPc molecules into the cavities within the experimental error. To our knowledge, CuPc is not known to form single component monolayers at the solid/liquid interface, the HBN network stabilises the CuPc molecules in a templating fashion. The diffuse image contrast of unoccupied cavities is nearly identical in intensity to the surrounding molecules (figure 1b inset). As the STM measurements were performed at the solid/liquid interface, presumably weakly bound **3,3'-BTP** molecules present in the supernatant liquid are adsorbed in the comparatively large cavities (see below). The high mobility (rotation) of those weakly bound co-adsorbed molecules results in the observed diffuse contrast. In the STM images of the CuPc/**3,3'-BTP** network, the  $D_{4h}$ -symmetry of the incorporated CuPc molecules is not recognisable, the guest molecules are imaged as bright disks. The  $C_{6h}$ -symmetry of the void and the  $D_{4h}$ -symmetry of the CuPc guest result in three energetically equivalent adsorption sites for CuPc in the cavity as indicated in figure 2. At room temperature, the CuPc molecules are thermally activated and rotate in the cavity. We performed force-field calculations using the Forcite module of the Materials Studio package where the host-guest network was modeled on a three-layer graphite (0001) slab within a 19x19 surface unit cell. Since most force fields do not allow for a square-planar coordinated Cu, the adsorption or stabilisation energy of CuPc could not be evaluated directly. Therefore we have computed the adsorption energy of phthalocyanine ( $PcH_2$ ) which will be very similar to the adsorption energy of CuPc as the binding occurs mainly via van der Waals forces and hydrogen bonds. An estimation of the rotation barrier of  $PcH_2$  within the void using the different force fields indicate that it should be of the order of  $E_a = 40 \text{ kJ}\cdot\text{mol}^{-1}$ . Assuming a rather low prefactor of  $k_0 = 1 \times 10^{10} \text{ s}^{-1}$  because of the large moment of inertia of the  $PcH_2$  molecule, a rate constant  $k = k_0 \exp(-E_a/K_B T) \sim 2,000 \text{ s}^{-1}$  at room temperature which means that the  $PcH_2$  molecules change their orientation about two thousand times per second. In these calculations, the solvent is not included, however, this should have little influence on the determination of the rotation barrier since the

effect of the solvent should be rather similar in the equilibrium configuration and at the barrier position. As the frequency of the rotation is higher than the scanning process, a CuPc molecule is imaged as a disk. A similar behaviour was observed at RT and in UHV for CuPc on a hexagonal  $C_{60}$  phase<sup>[14]</sup> and for the fourfold symmetric zinc-octaethylphorphyrin in a hexagonal molecular network.<sup>[15]</sup> A schematic summary of the theoretical calculation results of the host/guest-network on two graphite layers is shown in figure 2. The **3,3'-BTP** molecules are self-assembled into a  $C_{6h}$ -symmetric gearwheel-like structure, composed of six molecules in all three possible configurations (due to mirror symmetry along the lattice vectors) with respect to the lattice directions.

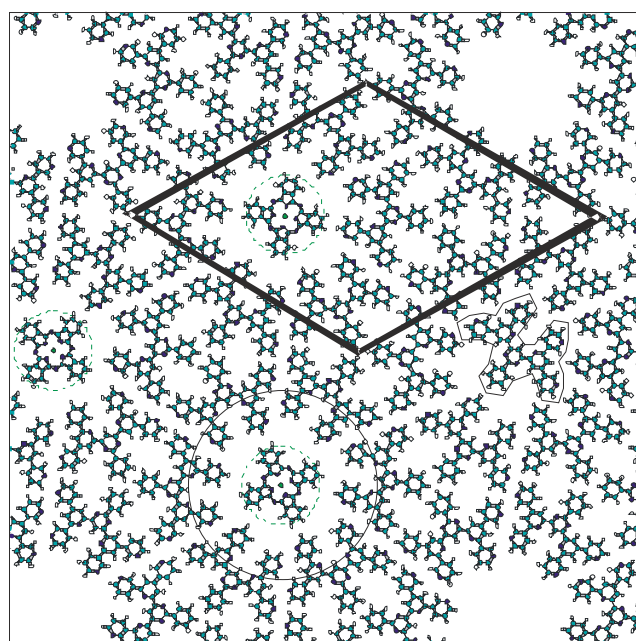


**Figure 2.** Molecular surface structure of the host-guest network. A single gearwheel is highlighted with a black circle. The host molecule **3,3'-BTP** is contoured black. CuPc in its three energetically equivalent adsorption configurations is highlighted green. At the solid/liquid-interface most of the cavities are occupied with co-adsorbed **3,3'-BTP** molecules.

The stabilisation energy of a phthalocyanine molecule in the host network was calculated with the UFF force field to  $404.3 \text{ kJ}\cdot\text{mol}^{-1}$  the corresponding value of a **3,3'-BTP** molecule was determined to  $467.9 \text{ kJ}\cdot\text{mol}^{-1}$  which is only slightly less than stabilisation energy of  $473.7 \text{ kJ}\cdot\text{mol}^{-1}$  of **3,3'-BTP** in the HBN. Similar results were obtained with other force fields. These stabilisation energies were determined with respect to the free molecules in the gas phase, i.e., the influence of the solvent is entirely neglected although the solvation energies in principle enter the expression for the stabilization energy. Therefore the calculated energies are only meant to give qualitative trends. In additional coadsorption experiments we observed neither a immobilisation of  $C_{60}$  nor coronene, both with significantly smaller stabilisation energies, calculated with the Dreiding force field in a trimesic acid network.<sup>[6]</sup> With these qualitatively similar stabilisation energies of CuPc and **3,3'-BTP** taken into account and the supposition that there is an equilibrium

between weakly adsorbed molecules and species dissolved in the supernatant liquid, we conclude an equilibrium between both components occupying the host cavities. Therefore the overall occupation with CuPc molecules should depend on the concentration of CuPc in the supernatant liquid.

The occupation of the host cavities in figure 3a, at a CuPc concentration of  $1.7 \cdot 10^{-5} \text{ mol} \cdot \text{L}^{-1}$  and a **3,3'-BTP** concentration of  $3 \cdot 10^{-5} \text{ mol} \cdot \text{L}^{-1}$  (together in ca.  $10 \mu\text{L}$ ) is approx. 16% and is not increasing with measuring time. A second addition ( $10 \mu\text{L}$ ) of the same CuPc solution after (almost) complete evaporation of the solvent from the first CuPc addition doubles the occupation to approx. 31% (figure 3b). An analysis of the short-range order of the adsorbed CuPc molecules revealed their random distribution in the cavities pointing to the fact that there are no significant interactions between guest molecules.<sup>[16]</sup> Thus, Langmuir-type adsorption isotherms are expected from which the equilibrium constants for CuPc and **3,3'-BTP** are determined to  $K_{\text{ads}}(\text{CuPc}) = (21.2 \pm 0.6) \cdot 10^4 \text{ L} \cdot \text{mol}^{-1}$  and  $K_{\text{ads}}(\text{BTP}) = (55.9 \pm 2.6) \cdot 10^4 \text{ L} \cdot \text{mol}^{-1}$  corresponding to adsorption enthalpies of  $-30.4 \pm 0.1 \text{ kJ mol}^{-1}$  and  $-32.8 \pm 0.1 \text{ kJ mol}^{-1}$ , respectively (supp. inf.). As predicted qualitatively by theory the stabilisation energy of **3,3'-BTP** molecules on HOPG is larger than that of the CuPc species (see above) but both are in the expected range of physisorption. According to these values an (almost) complete occupation of the cavities with CuPc (e.g.  $\Theta = 0.99$ ) can be achieved only with a concentration of at least approx.  $8 \cdot 10^{-3} \text{ mol} \cdot \text{L}^{-1}$  which exceeds by far the solubility of CuPc in TCB.

The low and adjustable occupation of the host network cavities gives already the possibility for non-selective manipulation but makes the CuPc/**3,3'-BTP**-system a perfect candidate for selective manipulation of individual guest molecules at the solid/liquid interface. The strong interaction of the large **BTP**  $\pi$ -system with the substrate and the strong intermolecular hydrogen bonds between individual physisorbed **BTP** molecules (supp. inf.) yield in a highly stable network. The mean resident time of a CuPc molecule in a host cavity was determined to  $435 \pm 20 \text{ s}$ , averaged over 97 CuPc molecules. While scanning with different imaging parameters (10 to 20 pA,  $-0.5$  to  $-1\text{V}$ ), we detected no noticeable alteration of the resident time. Compared to other systems with a quantified dynamic, the host-guest dynamic in the CuPc/**3,3'-BTP**-network is very slow.<sup>[17]</sup>

The selective tip controlled desorption of an individual CuPc molecule by a voltage pulse ( $+2 \text{ V}$ ,  $10 \mu\text{s}$ ) is shown in figure 4a. The process is selective to the CuPc molecule to which the tip is focused and successful within  $76 \pm 13\%$  of the manipulation events (supp. inf.). We did not observe the "refilling" of the emptied cavities with CuPc molecules in following images, but we can not exclude that the unsuccessful manipulation events are due to an immediate reoccupation of the cavity with CuPc subsequent to the manipulation process.

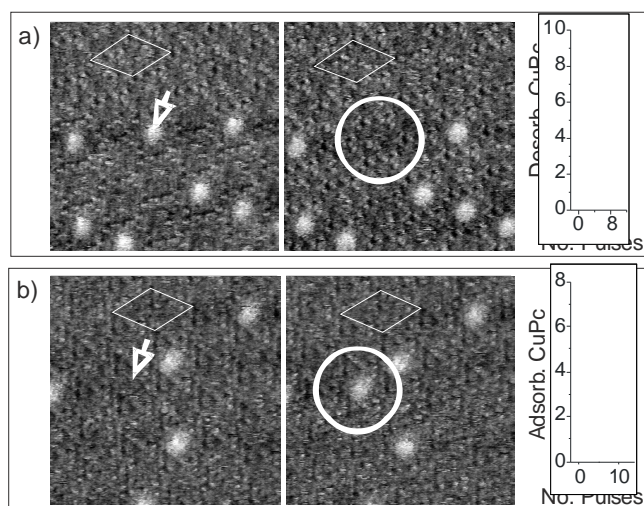


**Figure 4.** Subsequently recorded STM images and statistical analysis demonstrating the two manipulation experiments. The arrows indicate the tip position during applying the voltage pulse, the circles indicate the manipulated region. The rhombic unit cell of the host network is drawn for clarity. Image size is  $21.8 \text{ nm} \times 21.8 \text{ nm}$ . a) STM image sequence before and after "erasing" of an incorporated CuPc molecule from the gearwheel structure. Plot of the numbers of CuPc molecules desorbing after zero (intrinsic dynamics) and eight voltage pulses. Pulse intensity  $+2 \text{ V}$ ,  $10 \mu\text{s}$ . b) STM image sequence before and after "writing" of a CuPc molecule into a cavity of the host network. Pulse intensity  $-2 \text{ V}$ ,  $10 \mu\text{s}$ . Plot of the numbers of adsorbed CuPc molecules after zero and ten voltage pulses, comparing a CuPc concentration of  $1.7 \cdot 10^{-5} \text{ mol} \cdot \text{L}^{-1}$  (lightgrey) and  $3.5 \cdot 10^{-5} \text{ mol} \cdot \text{L}^{-1}$  (grey).

Besides the regioselective "erasing" of a single CuPc molecule, we were able to induce the CuPc adsorption into HBN cavities with defined voltage pulses ( $-2 \text{ V}$ ,  $10 \mu\text{s}$ ). The "writing" process for a single CuPc molecule is shown in figure 4 b). To induce the CuPc adsorption into the host network, a voltage pulse was applied to the tip focused on individual cavities. The image recorded immediately after the voltage pulse shows an additional bright spot (figure 4b), located at the same surface region where no bright spot was present in the former image. Unfortunately, the tip induced adsorption is not very selective to the aimed cavity due to the large tip-sample separation (approx.  $14 \text{ nm}$  ( $60 \text{ G}\Omega$ ) according to  $V = -0.7 V_{\text{Bias}}$  and  $I_{\text{T}} = 10 \text{ pA}$ ). In principle, the lateral resolution of our method is restricted to the next neighbour distance of the HBN cavities of about  $4.4 \text{ nm}$ . We estimated the mean lateral error of the tip induced deposition to  $10 \text{ nm}$  (2.3 times next neighbour distance). In both cases, "writing" and "erasing", the host network remains unaffected. To verify the tip induced desorption and adsorption, we separated the intrinsic dynamics of the host-guest network from the manipulation process. Therefore we compared the numbers of CuPc molecules adsorbing and desorbing with and without applying several voltage pulses. The results show a significant difference between the intrinsic dynamic and the tip induced adsorption and desorption (figure 4 and supp. inf.). The error bars are due to the intrinsic dynamic. Note that as the bimolecular system is in the thermodynamic equilibrium, the overall CuPc occupation remains similar before and after the manipulation process.

For the mechanism for the tip induced molecule desorption at the solid/liquid interface, we refer to an increased tip-molecule interaction at constant tip height,

controlled with a voltage pulse.<sup>[5]</sup> Increasing the tip-molecule interaction with a smaller tip-sample separation<sup>[6, 8]</sup> resulted in an uncontrolled perturbation of the host-guest network. However, the tip induced selective adsorption of a guest molecule into a host network cavity has not been observed before. We exclude the possibility of placing a CuPc molecule attached to the tip apex into the cavity with the voltage pulse. For this, the electronic and therefore imaging difference between a neat tip and a tip with a molecule adsorbed to the apex was not observed.<sup>[7]</sup> It is more likely that the molecule that gets adsorbed was previously in the solution. Thus, an increase of concentration of CuPc in the supernatant should increase the number of successful tip induced adsorption experiments which indeed could be shown (figure 4 and supp. inf.). We consider either trapping a CuPc molecule in the dielectric between the two electrodes or disturbing the equilibrium between immobilised **3,3'-BTP** and solvated CuPc molecules. These open questions are addressed in forthcoming experiments.

In summary, we reported on the reversible host-guest interaction of CuPc molecules with a hydrogen-bonded network of **3,3'-BTP** at the liquid/solid interface. Equilibrium constants of adsorption and corresponding adsorption enthalpies were determined. Furthermore, the tip induced adsorption and desorption of CuPc molecules is presented. The specific host-guest chemistry of the CuPc/**3,3'-BTP** HBN, referred to well balanced intermolecular interactions, and the controlled "writing" and "erasing" of individual guest molecules creates an opportunity to develop new functional nanomaterials. Ongoing experiments are dealing with fine tuning of the binary system towards the controlled formation of defined molecular structures with the presented method. Besides its own relevance as catalytic and electronic material CuPc has served in the present contribution as model compound within the huge class of phthalocyanines as further potential guest molecules in the **3,3'-BTP** network.

## Experimental Section

The investigated bis(terpyridine) derivative **3,3'-BTP** was synthesised as previously described.<sup>[2]</sup> Copper(II)phthalocyanine (CuPc) and 1,2,4-trichlorobenzene (TCB) were used as received from commercial sources. The STM measurements were performed at ambient conditions at the solid/liquid interface with a commercially available low-current RHK SPM1000 STM with a resolution of 1024 x 1024 data points per image and a scan speed between 600 nm/s for the host and host-guest network and 512 x 512 data points and 3 μm/s for the manipulation experiments. Generally, after cleaving the highly ordered pyrolytic graphite (HOPG) surface with adhesive tape, the quality of the mechanically cut Pt/Ir(80/20) tip was examined through atomic resolution of the graphite surface. The atomically resolved graphite images were used for calibration. After stopping the scanning process a drop of a solution of **3,3'-BTP** in TCB was applied to the surface with the tip in tunnel contact. After successfully imaging the **3,3'-BTP** network, a drop of a saturated solution of CuPc in TCB was applied to the surface. For the manipulation experiments, the scanning process was interrupted and the tip was located above the desired surface area. After the voltage pulses of preset intensity and duration were applied, the scanning process was immediately resumed. The tunneling current setpoint was between 10 to 20 pA, the bias voltage between -0.5 to -1 V. The tip controlled desorption was done with a 10 μs pulse of +2 V, the adsorption with a 10 μs pulse of -2 V. The presented STM images of the host-guest network were filtered to reduce noise and to enhance image contrast. The STM images of the host network have not been subject to image processing except slope subtraction.

Received: ((will be filled in by the editorial staff))

Published online on ((will be filled in by the editorial staff))

**Keywords:** scanning probe microscopy · host-guest systems · self-assembly · single molecule manipulation · porous network

- 
- [1] a) T. Yokoyama, S. Yokoyama, T. Kamikado, Y. Okuno, S. Mashiko, *Nature* **2001**, *413*, 619-621; b) S. B. Lei, C. Wang, S. X. Yin, H. N. Wang, F. Xi, H. W. Liu, B. Xu, L. J. Wan, C. L. Bai, *J. Phys. Chem. B* **2001**, *105*, 10838-10841; c) J. A. Theobald, N. S. Oxtoby, M. A. Phillips, N. R. Champness, P. H. Beton, *Nature* **2003**, *424*, 1029-1031; d) D. L. Keeling, N. S. Oxtoby, C. Wilson, M. J. Humphry, N. R. Champness, P. H. Beton, *Nano Lett.* **2003**, *3*, 9-12; e) S. Clair, S. Pons, A. P. Seitsonen, H. Brune, K. Kern, J. V. Barth, *J. Phys. Chem. B* **2004**, *108*, 14585-14590; f) M. Lackinger, S. Griessl, T. Markert, F. Jamitzky, W. M. Heckl, *J. Phys. Chem. B* **2004**, *108*, 13652-13655; g) M. Lackinger, S. Griessl, W. M. Heckl, M. Hietschold, G. W. Flynn, *Langmuir* **2005**, *21*, 4984-4988; h) S. Stepanow, N. Lin, F. Vidal, A. Landa, M. Ruben, J. V. Barth, K. Kern, *Nano Lett.* **2005**, *5*, 901-904; i) M. Stöhr, M. Wahl, C. H. Galka, T. Riehm, T. A. Jung, L. H. Gade, *Angew. Chem.* **2005**, *117*, 7560-7564; *Angew. Chem. Int. Ed.* **2005**, *44*, 7394-7398; j) L. Kampschulte, M. Lackinger, A.-K. Maier, R. S. K. Kishore, S. Griessl, M. Schmittel, W. M. Heckl, *J. Phys. Chem. B* **2006**, *110*, 10829-10836.
- [2] C. Meier, U. Ziener, K. Landfester, P. Wehrich, *J. Phys. Chem. B* **2005**, *109*, 21015-21027.
- [3] a) S. Griessl, M. Lackinger, M. Edelwirth, M. Hietschold, W. M. Heckl, *Single Mol.* **2002**, *3*, 25-31; b) J. Lu, S.-B. Lei, Q.-D. Zeng, S.-Z. Kang, C. Wang, L.-J. Wan, C.-L. Bai, *J. Phys. Chem. B* **2004**, *108*, 5161-5165; c) M. Ruben, D. Payer, A. Landa, A. Comisso, C. Gattinoni, N. Lin, J. P. Collin, J. P. Sauvage, A. De Vita, K. Kern, *J. Am. Chem. Soc.* **2006**, *128*, 15644-15651; d) N. Wintjes, D. Bonifazi, F. Cheng, A. Kiebele, M. Stöhr, T. Jung, H. Spillmann, F. Diederich, *Angew. Chem.* **2007**, *119*, 4167-4170; *Angew. Chem. Int. Ed.* **2007**, *46*, 4089-4092; e) M. Surin, P. Samori, *Small* **2007**, *3*, 190-194; f) S. Furukawa, K. Tahara, F. C. De Schryver, M. Van der Auweraer, Y. Tobe, S. De Feyter, *Angew. Chem.* **2007**, *119*, 2889-2892; *Angew. Chem. Int. Ed.* **2007**, *46*, 2831-2834; g) D. Bléger, D. Kreher, F. Mathevet, A.-J. Attias, G. Schull, A. Huard, L. Douillard, C. Fiorini-

- Debuischert, F. Charra, *Angew. Chem.* **2007**, *119*, 7548-7551; *Angew. Chem. Int. Ed.* **2007**, *46*, 7404-7407.
- [4] a) D. M. Eigler, E. K. Schweizer, *Nature* **1990**, *344*, 524-526; b) P. Zeppenfeld, C. P. Lutz, D. M. Eigler, *Ultramicroscopy* **1992**, *42-44*, 128-133; c) P. Samorí, H. Engelkamp, P. d. Witte, A. E. Rowan, R. J. M. Nolte, J. P. Rabe, *Angew. Chem.* **2001**, *113*, 2410-2412; *Angew. Chem. Int. Ed.* **2001**, *40*, 2348-2350.
- [5] A. Semenov, J. P. Spatz, M. Möller, J.-M. Lehn, B. Sell, D. Schubert, C. H. Weidl, U. S. Schubert, *Angew. Chem.* **1999**, *111*, 2701-2705; *Angew. Chem. Int. Ed.* **1999**, *38*, 2547-2550.
- [6] a) S. Griessl, M. Lackinger, F. Jamitzky, T. Markert, M. Hietschold, W. M. Heckl, *J. Phys. Chem. B* **2004**, *108*, 11556-11560; b) S. Griessl, M. Lackinger, F. Jamitzky, T. Markert, M. Hietschold, W. M. Heckl, *Langmuir* **2004**, *20*, 9403-9407.
- [7] M. Stöhr, M. Wahl, H. Spillmann, L. H. Gade, T. A. Jung, *Small* **2007**, *3*, 1336-1340.
- [8] L. Scudiero, K. W. Hipps, *J. Phys. Chem. C* **2007**, *111*, 17516-17520.
- [9] a) S. Kramer, R. R. Fuiere, C. B. Gorman, *Chem. Rev.* **2003**, *103*, 4367-4418; b) J. A. Williams, C. B. Gorman, *Langmuir* **2007**, *23*, 3103-3105.
- [10] a) D. Wouters, U. S. Schubert, *Angew. Chem.* **2004**, *116*, 2534-2550; *Angew. Chem. Int. Ed.* **2004**, *43*, 2480-2495; b) K. Salaita, Y. Wang, C. A. Mirkin, *Nat. Nano.* **2007**, *2*, 145-155.
- [11] a) C. B. Gorman, R. L. Carroll, Y. He, F. Tian, R. Fuiere, *Langmuir* **2000**, *16*, 6312-6316; b) J. Zhao, K. Uosaki, *Langmuir* **2001**, *17*, 7784-7788.
- [12] Manuscript in preparation
- [13] a) G.-B. Pan, X.-H. Cheng, S. Höger, W. Freyland, *J. Am. Chem. Soc.* **2006**, *128*, 4218-4219; b) E. Mena-Osteritz, P. Bäuerle, *Adv. Mater.* **2006**, *18*, 447-451.
- [14] M. Stöhr, T. Wagner, M. Gabriel, B. Weyers, R. Möller, *Phys. Rev. B* **2001**, *65*, 033404.
- [15] M. Wahl, M. Stöhr, H. Spillmann, T. A. Jung, L. H. Gade, *Chem. Comm.* **2007**, 1349-1351.
- [16] A. Bergbreiter, H. E. Hoster, S. Sakong, Groß, R. J. Behm, *Phys. Chem. Chem. Phys.* **2007**, *9*, 5127-5132.
- [17] G. Schull, L. Douillard, C. Fiorini-Debuischert, F. Charra, F. Mathevet, D. Kreher, A. J. Attias, *Nano Lett.* **2006**, *6*, 1360-1363.
-

**Entry for the Table of Contents** (Please choose one layout)

Layout 1:

**Host-Guest Chemistry**

((Author(s), Corresponding Author(s)\*))  
\_\_\_\_\_ **Page – Page**

((Title Text))

((Text for Table of Contents, max. 450 characters))

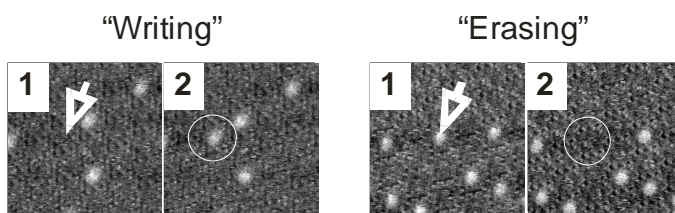
((TOC Graphic))

Layout 2:

**Host-Guest Chemistry**

Christoph Meier, Katharina Landfester,  
Daniela Künzel, Thomas Markert, Axel  
Groß, Ulrich Ziener\* \_\_\_\_\_  
**Page – Page**

Hierarchically Self-Assembled Host-Guest Network at the Solid/Liquid-Interface for Single Molecule Manipulation



**Manipulation at the solid/liquid interface:** A molecular monolayer polymorph of an oligopyridine forms a controllable host-guest network with copper(II)phthalocyanine at the solid/liquid interface. The slow dynamics of the guest molecules is utilised to manipulate individual guest molecules.

## Supporting Information

### Hierarchically Self-Assembled Host-Guest Network at the Solid/Liquid-Interface for Single Molecule Manipulation

Christoph Meier, Katharina Landfester, Daniela Künzel, Thomas Markert, Axel Groß, and Ulrich Ziener\*

#### Hydrogen bonded 3,3'-BTP host-Network

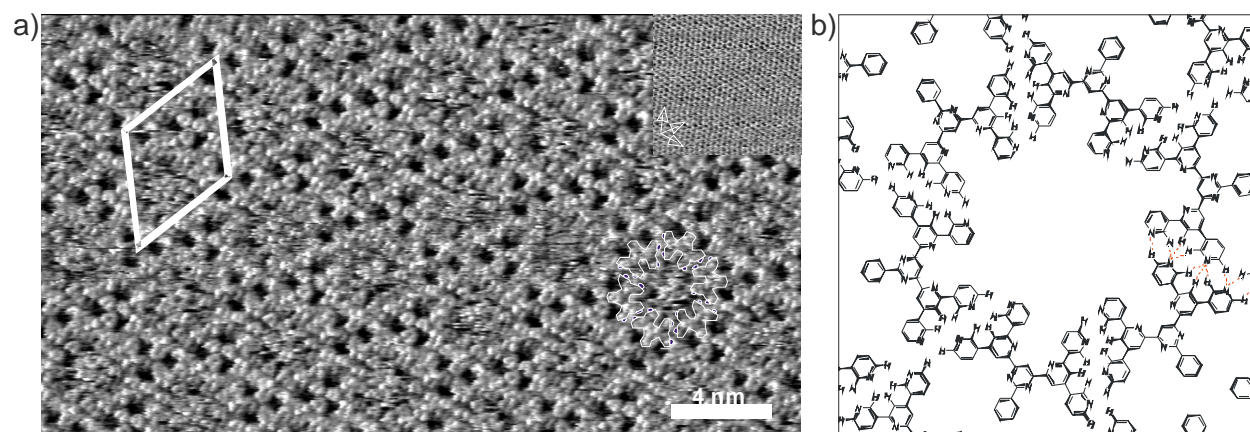


**Figure 1.** a) Submolecularly resolved STM picture of the gearwheel-like HBN structure of **3,3'-BTP** deposited on HOPG from a diluted TCB solution. The monolayer structure is characterised through three triangular ordered black depressions, separated by bright rings with a slight depression in their centre. Those ring-like fine structures can be ascribed to the phenyl rings of **BTP** molecules. The inset in the upper right corner shows the orientation of the under-lying graphite surface, the contour of a gearwheel composed of six **3,3'-BTP** molecules is drawn below. The lattice parameters of the rhombic unit cell were determined to  $a = b = 4.40 \pm 0.05$  nm, enclosing an angle of  $60 \pm 0.1^\circ$ . b) Hydrogen bonding pattern highlighted for a gearwheel composed of six oligopyridine molecules.

#### Mean Resident Time of CuPc in the HBN

The mean resident time  $t_{mean, resident}$  was calculated from the experimental resident times shown in table 1 with the following equation:

$$t_{resident, mean} = \frac{\sum \Delta n \cdot \Delta t}{\sum \Delta n}$$

**Table 1:** Resident times of individual CuPc molecules in the host network for the calculation of the mean resident time. Three image series were evaluated for the statistics. The time period  $\Delta t$  is given by the scan size and speed.  $n_{CuPc}$  is the total number of CuPc molecules in the tracked network region.  $\Delta n_{CuPc}$  is the number of CuPc molecules which have left their cavities after a certain time period.

$\Delta t$ [s]	1. series		2. series		3. series	
	$n_{CuPc}$	$\Delta n_{CuPc}$	$n_{CuPc}$	$\Delta n_{CuPc}$	$n_{CuPc}$	$\Delta n_{CuPc}$
0	47		26		24	
147	34	13	22	4	21	3
294	26	8	14	8	15	6
441	22	4	11	3	12	3
588	18	4	9	2	8	4
735	14	4	7	2	4	4
882	7	7	5	2	-	-
1029	7	1	-	-	-	-

The mean resident time was calculated to  $435 \pm 20$  s.

#### Langmuir Adsorption Isotherm

From different coverages  $\Theta$  at different concentrations  $c_0$  of oligopyridine **3,3'-BTP** and CuPc, respectively, the equilibrium constants  $K_{ads}$  were evaluated by fitting the experimental values with the program Origin 7.5<sup>®</sup> based on the equation of a Langmuir adsorption isotherm

$$\Theta(BTP) = \frac{K_{ads}(BTP) * c_{eq}(BTP)}{1 + K_{ads}(BTP) * c_{eq}(BTP)} \quad \text{and a modified equation for competing co-adsorption}$$

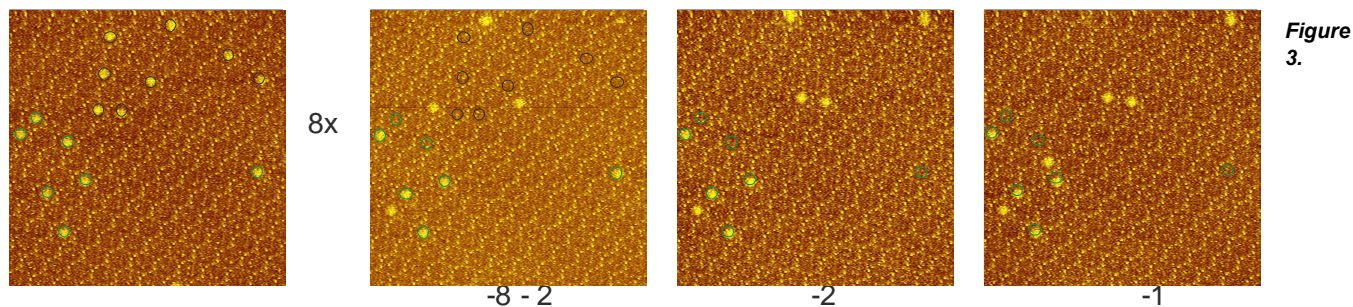
$$\Theta(CuPc) = \frac{K_{ads}(CuPc) * c_{eq}(CuPc)}{1 + K_{ads}(BTP) * c_{eq}(BTP) + K_{ads}(CuPc) * c_{eq}(CuPc)} \quad \text{with } c_0 \approx c_{eq}, \text{ justified by the fact that the amount of}$$

CuPc in solution is more than enough for a complete occupation of the host cavities (approx.  $1.5 \cdot 10^{12}$  cavities vs.  $1.0 \cdot 10^{14}$  CuPc molecules for a concentration of  $1.7 \cdot 10^{-5} \text{ mol} \cdot \text{L}^{-1}$  and a droplet volume of  $10 \mu\text{L}$ ). It is assumed that (i) there is no interaction between either of the adsorbing molecules, (ii) the host network is completely stable and non-dynamic in the respective concentration range, and (iii) solvent molecules do not adsorb.  $K_{ads}(BTP)$  determined from the first equation was used as constant in the second equation for the determination of  $K_{ads}(CuPc)$ .

**Figure 2.** Coverages of **3,3'-BTP** (left) and CuPc (right) in the HBN of **3,3'-BTP** on HOPG depending on the concentration at 298 K.

The free enthalpy of adsorption  $\Delta G_{ads}$  was determined according to  $\Delta G_{ads} = -RT \ln \frac{K_{ads}}{c^0}$ .

### Tip induced desorption



Representative STM image series showing the tip induced desorption of individual guest molecules as used for the statistical analysis. After recording the first image, a voltage pulse was applied to the tip placed above the CuPc molecules marked with black circles. The green circles indicate CuPc molecules which were not addressed. The third and fourth image were used to determine the intrinsic desorption of CuPc molecules. The numbers below the images are the numbers of CuPc molecules desorbing from the host-guest network relative to the previous image. CuPc concentration  $1.7 \cdot 10^{-5} \text{ mol} \cdot \text{L}^{-1}$ , image size  $50 \text{ nm} \times 50 \text{ nm}$ .

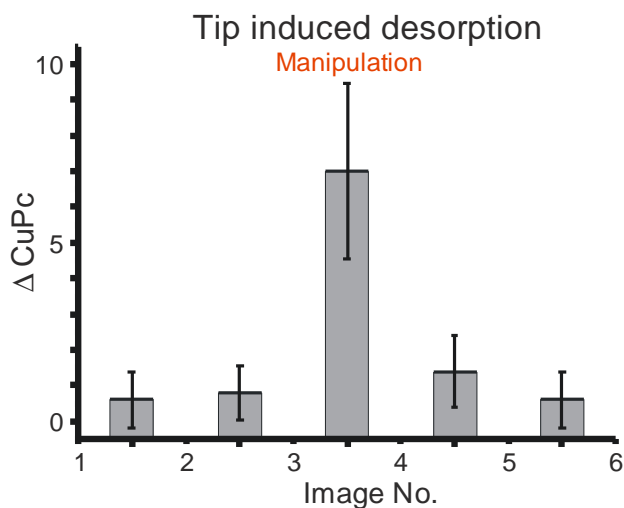


**Figure 4.** Statistical analysis of seven image sequences as shown in figure 3 considering the number of CuPc molecules leaving their host cavities in images before manipulation, immediately after manipulation and in images afterwards. The error bars are due to the intrinsic dynamics.

## Tip induced adsorption

a) CuPc  $1.7 \cdot 10^{-5} \text{ mol} \cdot \text{L}^{-1}$

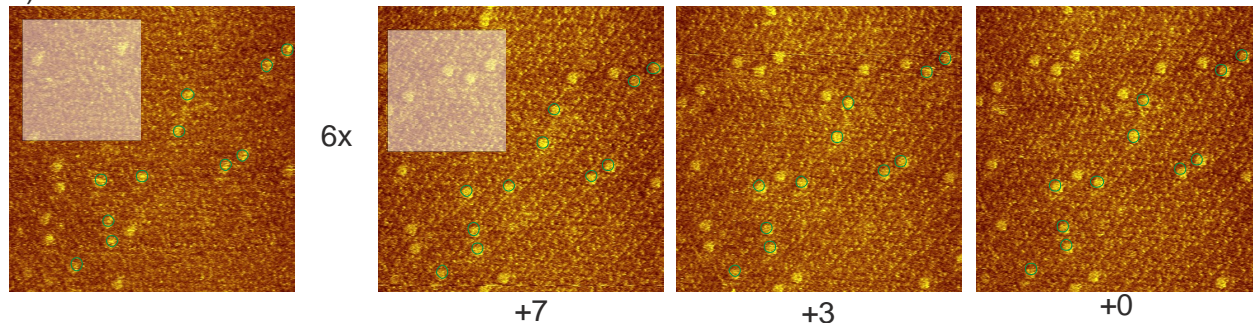
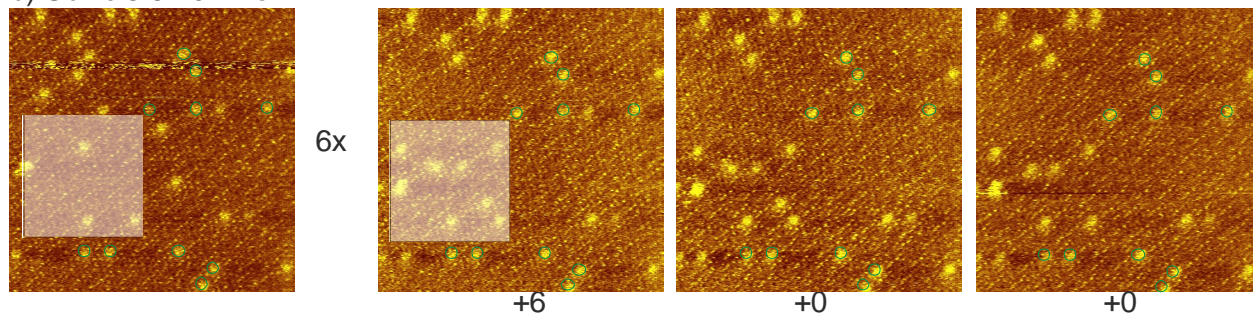


**Figure 5.**

b) CuPc  $3.5 \cdot 10^{-5} \text{ mol} \cdot \text{L}^{-1}$



Representative STM image series showing the tip induced adsorption of guest molecules as used for the statistical analysis. After recording the first image, a voltage pulse was applied to the tip placed above six individual cavities in the marked region. The green circles indicate some CuPc molecules which were used to verify the surface identity. The third and fourth images were used to determine the intrinsic adsorption of CuPc molecules. The numbers below the images are the numbers of CuPc molecules adsorbing into the host-guest network relative to the previous image. Image size 50 nm x 50 nm. a) Concentration of CuPc in the supernatant  $1.7 \cdot 10^{-5} \text{ mol} \cdot \text{L}^{-1}$ ; b) Concentration of CuPc in the supernatant  $3.5 \cdot 10^{-5} \text{ mol} \cdot \text{L}^{-1}$ .

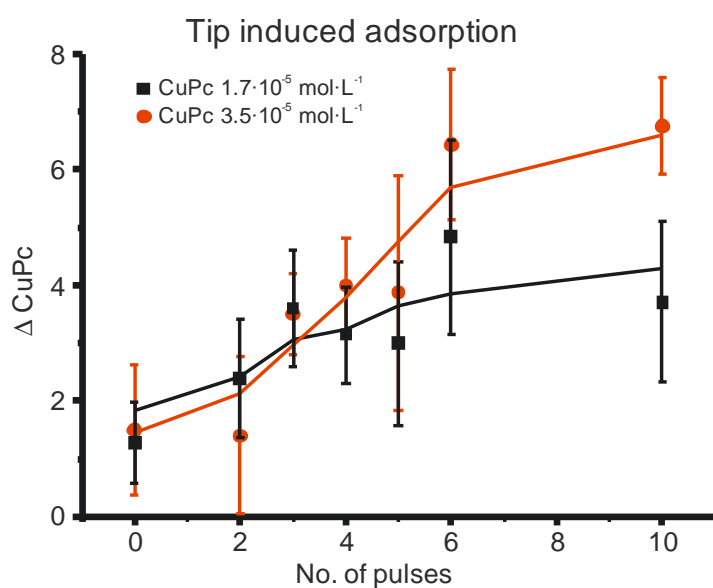


**Figure 6.** Statistical analysis of image sequences as shown in figure 3 considering the number of CuPc molecules adsorbing in host cavities without manipulation and after manipulation with a different number of voltage pulses for a CuPc concentration of  $1.7 \cdot 10^{-5} \text{ mol}\cdot\text{L}^{-1}$  and  $3.5 \cdot 10^{-5} \text{ mol}\cdot\text{L}^{-1}$ , respectively. Solid lines were fitted with a moving average of two points. The error bars are due to the intrinsic dynamics.